MedChemComm

RESEARCH ARTICLE

View Article Online
View Journal

Cite this: DOI: 10.1039/c5md00371g

1,3,4-Oxadiazole derivatives as potential antitumor agents: discovery, optimization and biological activity valuation

Yin Luo,†[a] Zhi-Jun Liu,†[a] Guo Chen,[b] Jing Shi,[a] Jing-Ran Li[a] and Hai-Liang Zhu*[a]

Received 30th August 2015,
Accepted 14th November 2015

DOI: 10.1039/c5md00371g

www.rsc.org/medchemcomm

Recent studies have proved that focal adhesion kinase (FAK) is a new potential therapeutic target in cancer therapy. In this study, a virtual screening was conducted to discover potential candidates for FAK inhibitors. Based on the results, a series of novel oxadiazole derivatives (**5a**–**5q**) bearing the benzotriazole group were designed and synthesized for FAK inhibitory evaluation. Among the compounds, **5h**, which has an *ortho* methoxy group on the benzene ring, exhibited the most potent inhibitory activity for cancer cell growth with an IC_{50} value of 11 μM and 0.250 μM against Hela cells and FAK, respectively. Further, the apoptosis assay indicated that compound **5h** induced the apoptosis of HeLa cells, and docking simulation showed that **5h** could bind to the FAK protein catalytic region. Taking these together, **5h** could be a lead for discovering novel FAK inhibitors.

1. Introduction

Cervical cancer is one of the major cancers worldwide with 12 360 new cases in the United States in 2014.[1] This cancer is a kind of malignant neoplasm arising from cells originating in the cervix uteri. Treatments for cervical cancer include surgery, chemotherapy and radiotherapy in the early and advanced stages. However, due to adverse effects or low efficiency, these treatment options for cervical cancer have not been satisfactory. Therefore, it is very important and needful to continuously develop new and potent agents for cervical cancer treatment.[2]

Focal adhesion kinase (FAK) is a kind of protein tyrosine kinase and located at specialized subcellular structures known as focal adhesions which link the extracellular matrix (ECM) to the cytoskeleton. FAK is a convergence point of a number of signal transduction pathways associated with cell adhesion, invasion, motility and angiogenesis.[3–6] FAK has been found to be overexpressed in most human cancers, particularly in highly invasive cancer cells.[7] Therefore, targeting FAK is a rational and novel approach to retard cancer growth and block metastasis.[8]

Since FAK was proposed to be a new potential therapeutic target in cancer therapy, several FAK inhibitors have been developed and reported recently. One of them, PF-573228, developed by Pfizer, selectively inhibited cancer cell motility but not cell growth and survival *in vitro*.[9] Another one, developed by Novartis, NVP-TAE226 (TAE226), inhibited glioma and ovarian tumor growth *in vivo*.[10–12] In this study, we aimed to develop new small molecule drugs targeting the FAK protein for treating cervical cancer. The availability of the crystal structure of FAK provides us an opportunity to utilize the virtual screening strategy to identify FAK inhibitors from our compound dataset, which contained most of the compounds synthesized and reported by our group. Based on the calculated binding affinity with the FAK structure which was generated from *in silico* screening, four hits (Table 1) were selected for initial protein kinase inhibitory activity test. Among them, Hit 2 containing the oxadiazole skeleton exhibited the best FAK inhibitory activity, with an IC_{50} value of 3.9 μM. Meanwhile, oxadiazoles are remarkably effective compounds with respect to their selective inhibitory activity for cancer cells. Previous studies showed that compounds containing the 1,3,4-oxadiazole skeleton exhibited a variety of biological activities, such as antitumor, anti-diabetic, antifungal and antibacterial activities.[13–17] Besides, benzotriazole derivatives have also been found to exhibit potential anti-mycobacterial, anti-tubercular and anti-inflammatory activities.[18–22]

Based on all of the above, in order to obtain more potent FAK inhibitors, various substitutions were introduced to the oxadiazole skeleton based on the structure of Hit 2. Seventeen benzotriazole derivatives with the oxadiazole skeleton were synthesized and evaluated for their FAK inhibitory activities.

[a] *State Key Laboratory of Pharmaceutical Biotechnology, Nanjing University, Nanjing 210023, People's Republic of China. E-mail: zhuhl@nju.edu.cn; Fax: +86 25 8968 2572; Tel: +86 25 8968 2572*
[b] *Department of Radiation Oncology, Emory University School of Medicine and Winship Cancer Institute of Emory University, Atlanta, GA 30322, USA*
† These two authors contributed equally to this paper.

Table 1 Initial virtual screening results and protein kinase inhibitory activities of selected "hits"

Compound	Structure	Binding free energies (ΔGb, kcal mol^{-1})	FAK inhibition IC_{50} (μM)
Hit 1	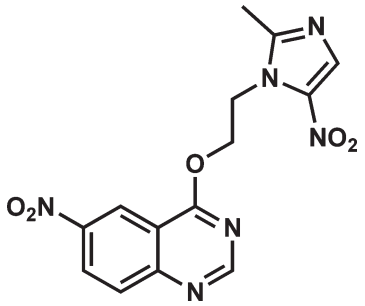	−24.75	10.4
Hit 2	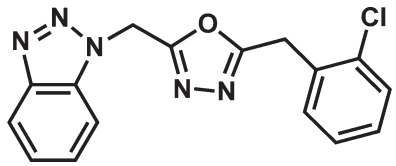	−25.32	3.9
Hit 3	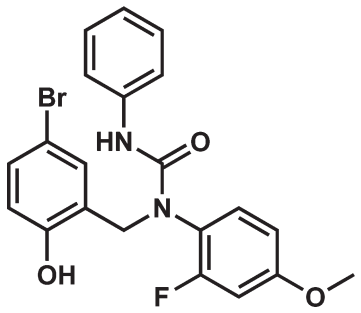	−25.29	26.5
Hit 4	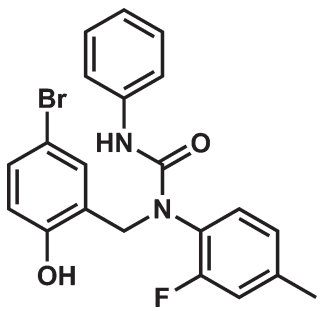	−24.68	10.63

Some compounds which exhibited favorable activities deserve further research as therapeutic agents for cervical cancer.

2. Results and discussion

2.1. Virtual screening

The LigandFit Dock protocol of Discovery Studio 3.1 was used to process *in silico* screening. The crystal structure of the FAK kinase domain with the inhibitor removed from the coordinates was downloaded from PDB database (PDB ID: 2ETM), and used as the receptor for compound binding. The ligand binding zones are structurally conserved very well at the level of the backbone and side chains. Amino acid residues within an appropriate radius around the compound were isolated to provide a sphere for docking simulation. This sphere was large enough to include every residue in the ATP-binding pocket of the FAK kinase domain. The binding affinity of candidate compounds was evaluated by the binding free energies. The compound which revealed the highest binding affinity was predicted to possess the lowest binding free energy. After screening our compound library, four initial hits were selected to undergo FAK inhibitory activity assay based on their binding affinities. Their chemical structures, predicted binding free energies and IC_{50} values are summarized in Table 1. The results indicated that Hit 2 having oxadiazole and benzotriazole groups exhibited the best activity with an IC_{50} value of 3.9 μM. However, Hit 1, Hit 3 and Hit 4 possessing calculated binding free energies comparable to Hit 2 did not show favorable FAK inhibitory activities. In order to get more potent compounds, we modified the structure of Hit 2 using a structure-based drug design. The aim of the modification was to generate a structure–activity relationship analysis for the oxadiazole and benzotriazole combined scaffold based compounds.

Table 2 Structures of oxadiazole derivatives (**5a–5q**)

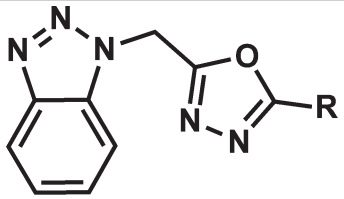

Compounds	R	Compounds	R
5a	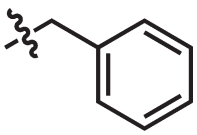	**5j**	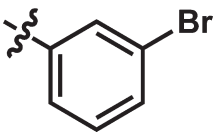
5b	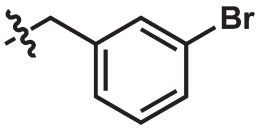	**5k**	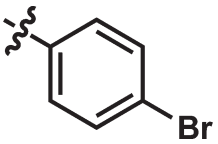
5c	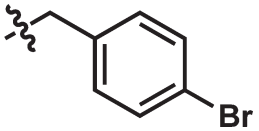	**5l**	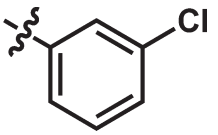
5d	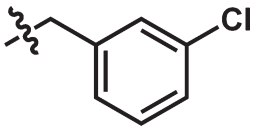	**5m**	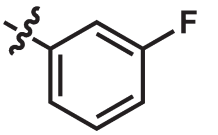
5e	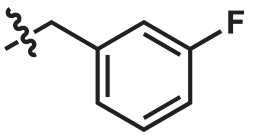	**5n**	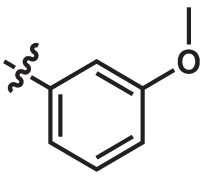
5f	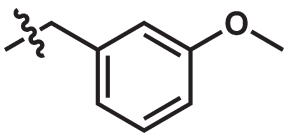	**5o**	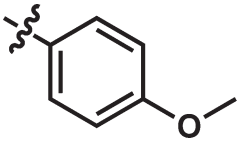
5g	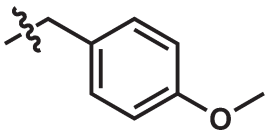	**5p**	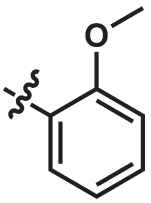
5h	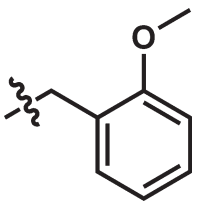	**5q**	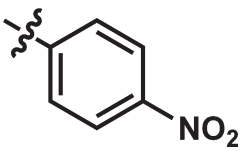
5i	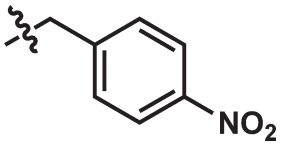		

2.2. Chemical synthesis

In this study, 17 oxadiazole derivatives **5a–5q** (Table 2) were synthesized, of which 14 were reported for the first time, and compounds **5k**, **5o** and **5q** have been reported before.[23–25] The synthetic route of the new oxadiazole derivatives was outlined in Scheme 1. The synthesis of these derivatives was started from benzene-1,2-diamine (**1**) with treatment of CH_3-COOH and $NaNO_2$ solution to give compound **2**. Compound **2** was then *N*-substituted with ethyl chloroacetate in methanol to give ethyl 1,2,3-benzo[*d*]triazol-1-ylacetate (**3**), which was hydrazinated by hydrazine hydrate affording 1,2,3-benzo[*d*]triazol-1-ylacetic hydrazide (**4**). Compound **4** was treated with different aromatic carboxylic acids in the presence of phosphoryl chloride to yield compound **5**. All of the synthetic compounds gave satisfactory analytical and spectroscopic data, which were in full accordance with depicted structures of the compounds.

2.3. Biological activity

2.3.1. Cytotoxicity assay. Sometimes, the inhibitory activities of compounds result from their toxic effects and consequently erroneous conclusions might be made. Prior to the following bioactivity analysis, all the synthesized oxadiazole derivatives were tested for their cytotoxicity on human macrophage *in vitro* to evaluate their potential toxicity. The results are summarized in Table 3. The data showed that most of the oxadiazole derivatives had quite low toxicity. Besides, our research group has synthesized another series of benzotriazole derivatives with the oxadiazole skeleton as FAK inhibitors.[26] We found that the oxadiazole derivatives **5a–5q** displayed lower cytotoxicity than the reported compounds in that paper.

2.3.2. Biological activity assay. Compounds **5a–5q** were evaluated for their antitumor activities against HeLa (human cervical carcinoma cell line), $HepG_2$ (human hepatoma cell line) and MCF-7 (human breast cancer cell line) cells, taking cisplatin, one of the most effective broad-spectrum anticancer drugs,[27] as the reference.

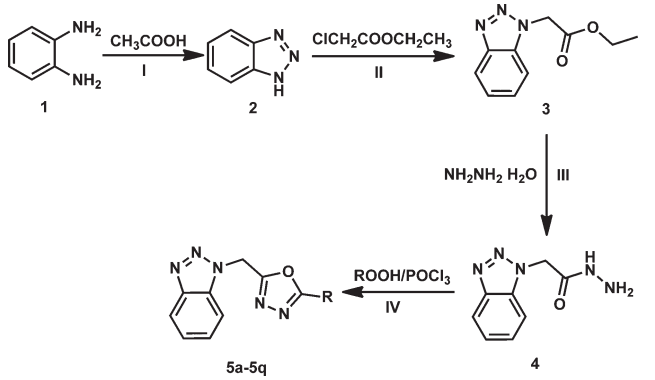

Scheme 1 Synthetic route of compounds **5a–5q**. Reagents: (I) $NaNO_2$ (10% aq.) solution, CH_3COOH, reflux, 2 h; (II) CH_3OH, $ClCH_2COOCH_2CH_3$, r. t. 3–4 h; (III) CH_3OH (99% aq.), $NH_2NH_2{,}H_2O$, reflux, 5–6 h; (IV) ROOH, $POCl_3$, reflux, 10–16 h.

As summarized in Table 3, most of the compounds showed certain effects against HeLa, $HepG_2$ and MCF-7 cell lines. By investigating the comparable selectivity of the tested compounds on these three cell lines, it was revealed that compounds **5a–5q** showed more potent effects against HeLa relative to the other two cell lines. Most significantly, compound **5h** displayed the most potent antitumor activity with an IC_{50} of 11 μM against HeLa cells, which was comparable to the activity of cisplatin (IC_{50} = 12 ± 1.1 μM for Hela cells). For HeLa cells, higher inhibitory activities were observed for all synthesized compounds with the IC_{50} values in the range of 11–328 μM. Compound **5h** also showed potent inhibitory activity against MCF-7 cells with an IC_{50} value of 16 μM which was even better than the most potent compound (IC_{50} = 16 μM) in our previous work.[22,23] The improvement of the antitumor activity proved that our structural optimization was effective.

Structure–activity relationship (SAR) analysis indicated that compounds with electron-donating groups on the benzene ring (*e.g.* **5f**, **5g** and **5h**) showed stronger activity than those with electron-withdrawing groups (*e.g.* **5c**, **5d** and **5e**). In further study of compounds with electron-withdrawing groups (*e.g.* **5b**, **5d**, **5e** and **5i**), it was clear that different substituents led to different antitumor activities. The potency order was F < Cl < Br < NO_2. Meanwhile, a comparison of the same substitution on different positions of the benzene ring revealed the following findings: when the compounds were methoxy-substituted derivatives, the potency order was *ortho* > *meta* > *para* (*e.g.* **5f**, **5g** and **5h**). Besides, compounds **5a–5i** with the phenyl-1,3,4-oxadiazole group had better inhibitory activities than compounds **5j–5q** with the benzyl-1,3,4-oxadiazole group. Among all the compounds, **5h** showed the best activity against HeLa cells when the substituent on the benzene ring was an *ortho* methoxy group.

2.3.3. FAK inhibitory activity assay. Next, the FAK inhibitory activity of **5a–5q** was tested. The results were summarized in Table 3. Most compounds displayed potent FAK inhibitory activity. Compound **5h** showed the most potent inhibitory activity with an IC_{50} value of 0.25 μM. According to the data in Table 3, compounds with electron-donating groups showed stronger activity than those with electron-withdrawing groups. Besides, compounds with the phenyl-1,3,4-oxadiazole group (**5a–5i**) displayed better activities than those with the benzyl-1,3,4-oxadiazole group (**5j–5q**). The FAK inhibitory activities agreed with the SAR analysis of the anticancer activities. This result suggested that the potent anticancer activities of the synthesized compounds were correlated with their FAK inhibitory activities. The analysis provided one orientation for further developing novel FAK inhibitors.

2.3.4. Apoptosis assay. Apoptosis has been considered as a major mechanism for anti-cancer drugs to kill cancer cells. The apoptosis level induced by compound **5h** through Annexin V/PI staining using flow cytometry (FCM) was then evaluated (Fig. 1). HeLa cells were treated with 0, 2, 10 and 50 μM compound **5h**, respectively, for 24 h. The increased apoptosis in HeLa cells was observed in a dose-dependent

Table 3 The antiproliferative activities of compounds **5a**–**5q** against tumor cells and FAK inhibitory activities

Compound	IC_{50} + SD (μM) HeLa[a]	HepG2[a]	MCF-7[a]	FAK[b]	CC_{50} ± SD[a] (μM) Macrophage
5a	167 ± 11	369 ± 8	258 ± 13	2.2 ± 0.2	>100
5b	182 ± 10	398 ± 9	269 ± 5	2.6 ± 0.1	>100
5c	198 ± 23	357 ± 5	277 ± 9	2.9 ± 0.1	>100
5d	230 ± 9	401 ± 11	292 ± 7	3.2 ± 0.2	>100
5e	237 ± 5	368 ± 9	357 ± 4	3.3 ± 0.1	>100
5f	123 ± 7	350 ± 7	241 ± 4	1.1 ± 0.1	>100
5g	150 ± 6	357 ± 9	251 ± 5	1.8 ± 0.5	>100
5h	11 ± 2	334 ± 5	15 ± 1	0.25 ± 0.02	>100
5i	157 ± 3	367 ± 10	253 ± 13	1.9 ± 0.3	>100
5j	301 ± 8	488 ± 5	382 ± 6	6.6 ± 0.2	>100
5k	305 ± 8	438 ± 9	387 ± 5	5.7 ± 0.2	>100
5l	327 ± 15	440 ± 5	390 ± 7	3.90 ± 0.1	>100
5m	332 ± 5	451 ± 7	398 ± 8	3.8 ± 0.1	>100
5n	243 ± 6	476 ± 13	370 ± 5	3.5 ± 0.2	>100
5o	269 ± 9	477 ± 9	376 ± 11	3.200 ± 0.1	>100
5p	216 ± 12	452 ± 7	331 ± 10	3.2 ± 0.1	>100
5q	299 ± 11	483 ± 5	13 ± 7	3.8 ± 0.2	>100
Cis-platinum	11 ± 1	15 ± 2	37 ± 3	0.03 ± 0	>100

[a] Inhibition of the growth of cancer cell lines. [b] Inhibition of FAK.

manner after treatment with compound **5h**, indicating that compound **5h** induced the apoptosis of anticancer stimulated HeLa cells.

2.3.5. Molecular docking. To gain a better understanding of the potency of **5a**–**5q** and guide further SAR studies, the interaction of these compounds with FAK was simulated by docking the compounds into the ATP binding site of FAK. The 3D structure of FAK was downloaded from PDB (ID: 2ETM). All docking runs were applied by the CDocker protocol of Discovery Studio 3.1. The docking calculation results are shown in Table 4.

The predicted binding free energy was used as the criterion for ranking. The selected poses of **5f**, **5g** and **5h** had an estimated binding free energy of −28.4, −28.1 and −29.4 kJ mol^{-1}, respectively. This might be the main reason why the potency order of methoxy substituted compounds was *ortho* > *meta* > *para*. The binding modes of **5h** and FAK are depicted in Fig. 2 and 3. The FAK protein catalytic region formed two interaction bonds with **5h**. The amino acid residues which had interactions with FAK are labeled in Fig. 2. **5h** was stabilized by a hydrogen bond between the methoxy group and ARG426 (distance = 3.1 Å) and a π–cation interaction between the oxadiazole ring and ILE428 (distance = 6.4 Å). Amino acid residues GLU506 and GLY502 were close to the benzotriazole ring which might lead to intermolecular forces. The space between the amino acid residues and

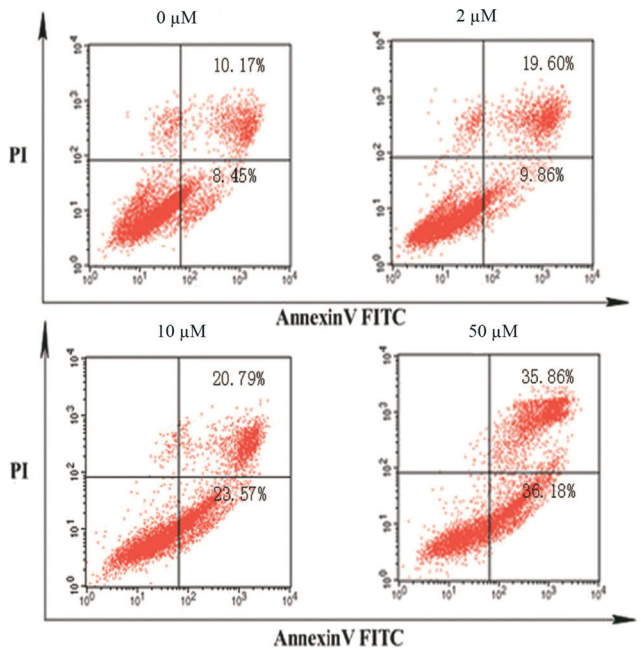

Fig. 1 Hela cells were cultured with various concentrations of **5h** for 24 h. Cells were stained by Annexin V FITC/PI. Apoptosis was analyzed by FCM.

Table 4 The docking calculation results of the synthesized compounds

Compounds	CDOCKER interaction energy, ΔGb (kJ mol^{-1})	Compounds	CDOCKER interaction energy, ΔGb (kJ mol^{-1})
5a	−28.55	**5k**	−26.89
5b	−26,96	**5l**	−25.32
5c	−27.10	**5m**	−25.18
5d	−26.97	**5n**	−26.97
5e	−26.78	**5o**	−26.87
5f	−28.44	**5p**	−27.11
5g	−28.13	**5q**	−26.98
5h	−29.41		
5i	−27.88		
5j	−26.54		

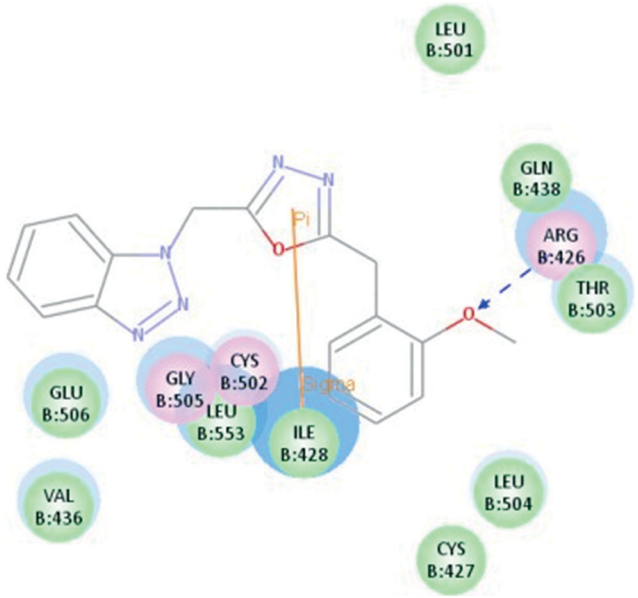

Fig. 2 2D ligand interaction diagram of compound **5h** with FAK protein (PDB ID: 2ETM). The essential amino acid residues at the binding site are tagged in circles. The purple circles show the amino acids which participated in hydrogen bonding, electrostatic or polar interactions. The green circles show the amino acids which participated in van der Waals interactions.

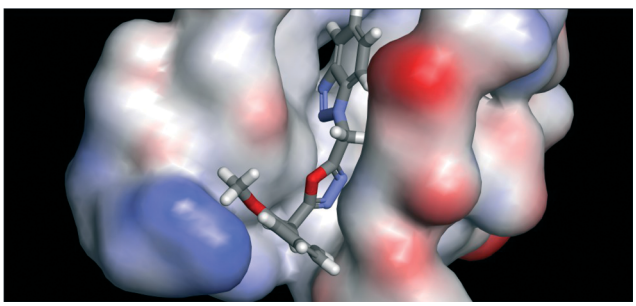

Fig. 3 3D model structure of the binding model of compound **5h** with FAK complex.

benzene ring was small. The molecular docking results showed that **5h** might be a direct binder of FAK.

3. Conclusions

A series of oxadiazole derivatives with the benzotriazole skeleton were synthesized and evaluated for their antiproliferative activities against three human cancer cell lines (HeLa, $HepG_2$ and MCF-7 cells). Preliminary results showed that some of the compounds displayed significant anticancer activities. Compound **5h** showed the most potent inhibitory activity with an IC_{50} value of 10.8 μM against HeLa cells, 334.2 μM against $HepG_2$ cells and 15.5 μM against MCF-7 cells. In order to predict the probable binding model of the kinase-inhibitor, molecular docking of the most potent inhibitor **5h** into the binding site of FAK was performed based on the FAK-inhibitor complex structure. It was found that several interactions of this compound with the amino acid residues in the binding site might play a crucial role in its FAK inhibition activity. This work might be helpful for the design and synthesis of anticancer agents with more potent activity.

4. Experimental section

4.1 Chemistry

The starting materials were obtained from commercial suppliers and used with or without purification as needed. Melting points were determined by an open capillary method on a 'Veego' VMP-D apparatus and are uncorrected. ^{1}H NMR spectra were recorded on a Varian Mercury (300 MHz) spectrometer in DMSO-d_6 with tetramethylsilane (TMS) as an internal standard and values were expressed in δ. Elemental analyses were performed for C, H, N and found within ±0.4% of theoretical values.

4.1.1 General procedure for synthesis of compound 2. To a solution of benzene-1,2-diamine (541 mg, 5 mmol) in CH_3-COOH (10 mL), $NaNO_2$ aq. soln. (25 mL, 1 M) was added and the solution was stirred at 70–80 °C for 2 h. Then the pH value was adjusted to 4.4–4.6 with 40% NaOH aq. soln. and 1 M HCl. The precipitated product was collected by filtration, washed with 5% ice NaCl aq. and recrystallized (CH_2Cl_2/CH_3OH) to afford compound **2** as a white powder.

4.1.2 General procedure for synthesis of compound 3. Benzotriazole (50 mmol) was dissolved in dry acetone (100 ml) and then anhydrous potassium carbonate (50 mmol) was added. After that, ethyl chloroacetate (50 mmol) was added, and then refluxed for 3–4 h. The reaction was monitored by TLC. Afterwards, the filtered reaction solution was evaporated under reduced pressure distillation to give the crude product. The crude product was purified by column chromatography [eluent: V (petroleum ether): V(ethyl acetate) = 9 : 1] to give a white solid (compound **3**).

4.1.3 General procedure for synthesis of compound 4. To a solution of compound **3** (20 mmol) in methanol, 85% hydrazine hydrate (80 mmol) was added and the solution was refluxed for 5–6 h. Then the appearing solid was filtered. The residue was recrystallized from ethanol to obtain compound **4**. Yield 56%, m. p. 89–91 °C, ^{1}H-NMR (300 MHz, DMSO-d_6, δ ppm): 3.54 (s, 2H), 4.62 (s, 2H), 7.23–7.69 (m, 4H), 8.05 (s, 1H). MS (ESI): 191.1 ($[M + H]^+$). Anal. calc. for $C_8H_9N_5O$: C, 50.26; H, 4.74; N, 36.63%; found: C, 50.27; H, 4.72; N, 36.64%.

4.1.4 General procedure for synthesis of compound 5a–5q. An equimolar mixture of compound **4** (1 mmol) and substituted carboxylic acid in phosphoryl chloride was refluxed for 10–16 h. Then the reaction mixture was cooled, poured into ice-cold water and neutralized with 20% $NaHCO_3$ solution. The resultant solid was filtered, washed with water and recrystallized from ethanol to give the title compound.

4.1.5 2-((1*H*-Benzo[*d*][1,2,3]triazol-1-yl)methyl)-5-benzyl-1,3,4-oxadiazole (5a). White powder, yield 63%, m. p. 230–232 °C. ^{1}H-NMR (300 MHz, DMSO-d_6, δ ppm): 4.03–4.17 (s, 2H), 5.43–5.57 (s, 2H), 7.21–7.24 (m, 1H), 7.17–7.29 (m, 4H), 7.29–7.35(m, 1H), 7.35–7.38 (m, 2H), 7.40–7.43 (m, 2H) MS (ESI):

291.31 ([M + H]$^+$). Anal. calc. for $C_{16}H_{13}N_5O$: C, 65.97; H, 4.50; N, 24.04%; found: C, 65.60; H, 4.52; N, 24.03%.

4.1.6 2-((1*H*-Benzo[*d*][1,2,3]triazol-1-yl)methyl)-5-(3-bromobenzyl)-1,3,4-oxadiazole (5b). White powder, yield 54%, m. p. 242 °C. ^{1}H-NMR (300 MHz, DMSO-d$_6$, δ ppm): 4.27 (s, 2H), 6.37 (s, 2H), 7.28–7.29 (m, 2H), 7.44–7.45 (m, 1H), 7.46–7.84 (m, 2H), 7.57–7.59 (m, 2H), 8.07–8.10 (d, J = 8.37 Hz, 1H) MS (ESI): 370.20 ([M + H]$^+$). Anal. calc. for $C_{16}H_{12}BrN_5O$: C, 51.91; H, 3.27; N, 18.92%; found: C, 51.94; H, 3.31; N, 18.89.

4.1.7 2-((1*H*-Benzo[*d*][1,2,3]triazol-1-yl)methyl)-5-(4-bromobenzyl)-1,3,4-oxadiazole (5c). White powder, yield 66%, m. p. 230–232 °C. ^{1}H-NMR (300 MHz, DMSO-d$_6$, δ ppm): 4.65 (s, 2H); 6.39 (s, 2H), 7.25–7.31 (m, 2H), 7.44–7.45 (m, 2H), 7.48–7.50 (d, J = 7.27 Hz, 2H), 8.06–8.10 (m, 2H). MS (ESI): 370.20 ([M + H]$^+$). Anal. calc. for $C_{16}H_{12}BrN_5O$: C, 51.91; H, 3.27; N, 18.92%; found: C, 51.90; H, 3.28; N, 18.91%.

4.1.8 2-((1*H*-Benzo[*d*][1,2,3]triazol-1-yl)methyl)-5-(3-chlorobenzyl)-1,3,4-oxadiazole (5d). White powder, yield 62%, m. p. 235–237 °C. ^{1}H-NMR (300 MHz, DMSO-d$_6$, δ ppm): 4.67(s, 2H), 6.08 (s, 2H), 7.38–7.45 (m, 2H), 7.54–7.59 (m, 3H), 7.66–7.70 (m, 1H), 8.04–8.07 (m, 2H). MS (ESI): 325.75 ([M + H]$^+$). Anal. calc. For $C_{16}H_{12}ClN_5O$: C, 58.99; H, 3.71; N, 21.50%; found: C, 56.01; H, 3.73; N, 21.48%.

4.1.9 2-((1*H*-Benzo[*d*][1,2,3]triazol-1-yl)methyl)-5-(3-fluorobenzyl)-1,3,4-oxadiazole (5e). White powder, yield 67%, m. p. 240–242 °C. ^{1}H-NMR (300 MHz, DMSO-d$_6$, δ ppm): 4.38(s, 2H), 5.79 (s, 2H), 7.22–7.38 (m, 5H), 7.43–7.52 (m, 1H), 7.55–7.58(m, 1H), 8.03–8.06 (m, 1H). MS (ESI): 309.30 ([M + H]$^+$). Anal. calc. for $C_{16}H_{12}FN_5O$: C, 62.13; H, 3.91; N, 22.64%; found: C, 62.14; H, 3.90; N, 22.66%.

4.1.10 2-((1H-Benzo[*d*][1,2,3]triazol-1-yl)methyl)-5-(3-methoxybenzyl)-1,3,4-oxadiazole (5f). White powder, yield 60%, m. p. 240–242 °C. ^{1}H-NMR (300 MHz, DMSO-d$_6$, δ ppm): 4.38(s, 2H), 4.56 (s, 3H), 5.79 (s, 2H), 6.83–6.86 (m, 3H), 7.17–7.20 (m, 3H), 7.38–7.40 (m, 1H), 7.43–7.54 (m, 1H). MS (ESI): 321.33 ([M + H]$^+$). Anal. calc. for $C_{17}H_{15}N_5O_2$: C, 63.54; H, 4.71; N, 21.79%; found: C, 63.50; H, 4.73; N, 21.80%.

4.1.11 2-((1*H*-Benzo[*d*][1,2,3]triazol-1-yl)methyl)-5-(4-methoxybenzyl)-1,3,4-oxadiazole (5g). White powder, yield 59%, m. p. 169–170 °C. ^{1}H-NMR (300 MHz, DMSO-d$_6$, δ ppm): 4.51(s, 2H), 4.72 (s, 3H), 5.26 (s, 2H), 6.81–6.84 (m, 2H), 7.06–7.09 (m, 3H), 7.42–7.45 (m, 3H). MS (ESI): 321.33 ([M + H]$^+$). Anal. calc. for $C_{17}H_{15}N_5O_2$:C, 63.54; H, 4.71; N, 21.79%; found: C, 63.51; H, 4.73; N, 21.80%.

4.1.12 2-((1*H*-Benzo[*d*][1,2,3]triazol-1-yl)methyl)-5-(2-methoxybenzyl)-1,3,4-oxadiazole (5h). White powder, yield 54%, m. p. 170–172 °C. ^{1}H-NMR (300 MHz, DMSO-d$_6$, δ ppm): 4.78(s, 2H), 4.91 (s, 3H), 5.23 (s, 2H), 6.42–6.44 (m, 2H), 7.09–7.14 (m, 4H), 7.46–7.54 (m, 3H), 8.01–8.20 (m, 1H). MS (ESI): 307.11([M + H]$^+$). Anal. calc. for $C_{16}H_{13}N_5O_2$: C, 62.53; H, 4.26; N, 22.79%; found: C, 62.56; H, 4.28; N, 22.77%.

4.1.13 2-((1*H*-Benzo[*d*][1,2,3]triazol-1-yl)methyl)-5-(4-nitrobenzyl)-1,3,4-oxadiazole (5i). White powder, yield 50%, m. p. 235–237 °C. ^{1}H-NMR (300 MHz, DMSO-d$_6$, δ ppm): 4.76 (s, 2H), 5.65 (s, 2H), 7.57–7.60 (m, 1H), 7.83–7.86 (m, 2H), 8.04–8.07 (m, 2H), 8.14–8.21(m, 3H). MS (ESI): 336.30 ([M + H]$^+$). Anal. calc. for $C_{16}H_{12}N_6O_3$: C, 57.14; H, 3.60; N, 24.99; O, 14.27%; found: C, 57.18; H, 3.58; N, 25.01%.

4.1.14 2-((1*H*-Benzo[*d*][1,2,3]triazol-1-yl)methyl)-5-(3-bromophenyl)-1,3,4-oxadiazole (5j). White powder, yield 70%, m. p. 235–237 °C. ^{1}H-NMR (300 MHz, DMSO-d$_6$, δ ppm): 5.57 (s, 2H), 7.28–7.41 (m, 2H), 7.44–7.48 (m, 2H), 7.49–7.50 (m, 3H); 8.09–8.10 (m, 1H). MS (ESI): 356.18 ([M + H]$^+$). Anal. calc. for $C_{15}H_{10}BrN_5O$: C, 50.58; H, 2.83; N, 19.66%; found: C, 50.56; H, 2.80; N, 19.69%.

4.1.15 2-((1*H*-Benzo[*d*][1,2,3]triazol-1-yl)methyl)-5-(4-bromophenyl)-1,3,4-oxadiazole (5k). White powder, yield 71%, m. p. 240–242 °C. ^{1}H-NMR (300 MHz, DMSO-d$_6$, δ ppm): 5.56 (s, 2H), 7.42–7.81 (m, 3H), 7.81–7.86 (m, 4H), 8.80–8.81(m, 1H). MS (ESI): 366.01 ([M + H] $^+$). Anal. calc. For $C_{15}H_{10}BrN_5O$: C, 55.90; H, 3.13; N, 26.08%; found: C, 55.92; H, 3.15; N, 26.30%.

4.1.16 2-((1*H*-Benzo[*d*][1,2,3]triazol-1-yl)methyl)-5-(3-chlorophenyl)-1,3,4-oxadiazole (5l). White powder, yield 65%, m. p. 240–242 °C. ^{1}H-NMR (300 MHz, DMSO-d$_6$, δ ppm): 6.09 (s, 2H), 7.09–7.15 (m, 3H), 7.17–7.44 (m, 1H), 7.65 (d, J = 7.64 Hz, 2H), 7.82 (d, J = 8.14, 2H). MS (ESI): 332.05 ([M + H]$^+$). Anal. calc. for $C_{16}H_{13}NO_5S$: C, 58.00; H, 3.95; N, 4.23%; found: C, 58.02; H, 3.97; N, 4.26%.

4.1.17 2-((1H-Benzo[*d*][1,2,3]triazol-1-yl)methyl)-5-(3-fluorophenyl)-1,3,4-oxadiazole (5m). White powder, yield 56%, m. p. 230–232 °C. ^{1}H-NMR (300 MHz, DMSO-d$_6$, δ ppm): 5.63 (s, 2H), 7.39–7.46 (m, 2H), 7.54–7.62 (m, 3H), 7.70–7.73 (m, 1H), 8.04–8.07 (m, 2H). MS (ESI): 346.37 ([M + H]$^+$). Anal. calc. for $C_{15}H_{10}FN_5O$, C, 61.02; H, 3.41; N, 23.72; O, 5.42%, found: C, 61.04; H, 3.39; N, 23.74%.

4.1.18 2-((1*H*-Benzo[*d*][1,2,3]triazol-1-yl)methyl)-5-(3-methoxyphenyl)-1,3,4-oxadiazole (5n). White powder, yield 62%, m. p. 235–237 °C. ^{1}H-NMR (300 MHz, DMSO-d$_6$, δ ppm): 3.45 (s, 2H), 5.43 (s, 2H), 7.16–7.21(m, 1H), 7.21–7.52 (m, 2H), 7.71–7.80 (m, 3H), 8.07–8.14 (m, 2H). MS (ESI): 307.31 ([M + H]$^+$). Anal. calc. for $C_{16}H_{13}N_5O_2$: C, 62.53; H, 4.26; N, 22.79%; found: C, 62.54; H, 4.24; N, 22.80%.

4.1.19 2-((1*H*-Benzo[*d*][1,2,3]triazol-1-yl)methyl)-5-(4-methoxyphenyl)-1,3,4-oxadiazole (5o). White powder, yield 70%, m. p. 230–232 °C. ^{1}H-NMR (300 MHz, DMSO-d$_6$, δ ppm): 3.81 (s, 3H), 5.08 (s, 2H), 7.23–7.55 (m, 3H), 7.65–7.78 (m, 2H), 7.90–8.07 (m, 1H), 8.15–8.34(m, 2H). MS (ESI): 307.31 ([M + H]$^+$). Anal. calc. for $C_{16}H_{13}N_5O_2$: C, 62.53; H, 4.26; N, 22.79%; found: C, 62.52; H, 4.29; N, 22.80%.

4.1.20 2-((1*H*-Benzo[*d*][1,2,3]triazol-1-yl)methyl)-5-(2-methoxyphenyl)-1,3,4-oxadiazole (5p). White powder, yield 64%, m. p. 230–232 °C. ^{1}H-NMR (300 MHz, DMSO-d$_6$, δ ppm): 3.89 (s, 3H), 5.23 (s, 2H), 7.12–7.23 (m, 1H), 7.23–7.44 (m, 3H), 7.55–7.75 (m, 2H), 7.77–7.96 (m, 1H), 8.10–8.12 (m, 2H). MS (ESI): 307.31 ([M + H]$^+$). Anal. calc. for $C_{16}H_{13}N_5O_2$: C 62.53; H, 4.26; N, 22.79%; found: C, 62.55; H, 4.28; N, 22.80%.

4.1.21 2-((1*H*-Benzo[*d*][1,2,3]triazol-1-yl)methyl)-5-(4-nitrophenyl)-1,3,4-oxadiazole (5q). White powder, yield 63%, m. p.

240–242 °C. ^{1}H-NMR (300 MHz, DMSO-d_6, δ ppm): 5.37 (s, 2H), 7.27–7.31 (m, 2H), 7.42–7.45 (m, 2H), 8.07–8.10 (m, 2H), 8.24–8.27 (m, 2H). MS (ESI): 411.96 ([M + H]$^+$). Anal. calc. for $C_{15}H_{10}BrN_5O$: C, 50.58; H, 2.83; N, 19.66%; found: C, 50.57; H, 2.85; N, 19.68%.

4.2 Biology

4.2.1 Antiproliferative assay. The antitumor activities of compounds **5a–5q** against the three cell lines HeLa, $HepG_2$ and MCF-7 were evaluated using a standard MTT-based colorimetric assay (Sigma). Briefly, cell lines were seeded at a density of 7×10^3 cells per well in 96-well microtiter plates (Costar). After 24 h, exponentially growing cells were exposed to the indicated compounds at final concentrations ranging from 0.1 to 500 μM. The indicated compounds were dissolved in PBS and DMSO (DMSO accounted for 0.4% in the solvent system). Negative control also used the PBS and DMSO solvent system. After 24 h, cell survival was determined by the addition of an MTT solution (10 μL of 5 mg mL^{-1} MTT in PBS). After 4 h, 100 μL of 10% SDS in 0.01 N HCl was added, and the plates were incubated at 37 °C for a further 18 h; optical absorbance was measured at 570 nm on an LX300 Epson Diagnostic microplate reader. Survival ratios are expressed in percentages with respect to untreated cells. IC_{50} values were determined from replicates of six wells from at least three independent experiments.

4.2.2 FAK inhibition assay. Seventeen 1,3,4-oxadiazole derivatives were tested in a search for small molecule inhibitors of FAK. In a typical study, human recombinant full-length FAK was incubated in a kinase buffer containing ATP and the substrate for 4 h at room temperature with or without the presence of the oxadiazole derivatives. The final concentration of the drug was set as 50, 10, 2, 0 μg mL^{-1}, respectively. The remaining ATP in solution was then quantified utilizing the Kinase-Glo-luminescence kit (Promega).

4.2.3 Apoptosis assay. For Annexin V/PI assays, cells were stained with Annexin V FITC and PI and then monitored for apoptosis by flow cytometry. Briefly, 0.5×10^6 cells were washed with PBS and stained with 5 μL of Annexin V-FITC and 2.5 μL of PI (5 μg mL^{-1}) in a binding buffer (10 mM HEPES, pH 7.4, 140 mM NaOH, 2.5 mM $CaCl_2$) for 30 min at room temperature in the dark. Apoptotic cells were quantified using a FACS can cytofluorometer (PT. Madagasi Brosa Inc. Jl. Batang Hari No. 73, Propinsi Sumatera Utara, Indonesia). Statistical analysis was performed using WINMDI software version 2.8 (The Scripps Research Institute (TSRI), San Diego, CA, USA). Both early apoptotic (Annexin V positive and PI negative) and late apoptotic (double positive of Annexin V and PI) cells were detected.

4.2.4 Docking simulations. Molecular docking of compounds into the three dimensional X-ray structure of the FAK catalytic subunit (PDB code: 2ETM) was carried out using Discovery Studio (version 3.1) as implemented through the graphical user interface Discovery Studio CDOCKER protocol.

The three-dimensional structures of the aforementioned compounds were constructed using ChemBio 3D Ultra 11.0 software [Chemical Structure Drawing Standard; Cambridge Soft corporation, USA (2008)], then they were energetically minimized by using MMFF94 with 5000 iterations and a minimum RMS gradient of 0.10. The crystal structures of the FAK catalytic subunit were retrieved from the RCSB Protein Data Bank (http://www.rcsb.org/pdb/home/home.-do). All bound water and ligands were eliminated from the protein and polar hydrogen was added. The whole 2ETM was defined as a receptor and the site sphere was selected based on the active center of 2ETM according to a previous report, then compounds were placed during the molecular docking procedure. The types of interactions of the docked protein with the ligand were analyzed after the end of molecular docking.

Acknowledgements

This work was supported by Jiangsu Planned Projects for Postdoctoral Research Funds (1302007C), China Postdoctoral Science Foundation Funds (2014M551563) and International Postdoctoral Exchange Fellowship Program (20130023).

Notes and references

1 R. Siegel, J. Ma, Z. Zou and A. Jemal, *Ca-Cancer J. Clin.*, 2014, **64**, 9–29.
2 V. Kumar, A. K. Abbas, N. Fausto and R. N. Mitchell, *Robbins Basic Pathology*, Saunders Elsevier, 8th edn, 2007, pp. 718–721.
3 B. D. Cox, M. Natarajan, M. R. Stettner and C. L. Gladson, *J. Cell. Biochem.*, 2006, **99**, 35–52.
4 S. M. Frisch, K. Vuori, E. Ruoslahti and P. Y. Chan-Hui, *J. Cell Biol.*, 1996, **134**, 793–799.
5 D. D. Schlaepfer, S. K. Mitra and D. Ilic, *Biochim. Biophys. Acta*, 2004, **1692**, 77–102.
6 V. M. Golubovskaya and W. G. Cance, *Int. Rev. Cytol.*, 2007, **263**, 103–153.
7 V. Gabarra-Niecko, M. D. Schaller and J. M. Dunty, *Cancer Metastasis Rev.*, 2003, **22**, 359–374.
8 G. W. McLean, N. O. Carragher, E. Avizienyte, J. Evans, V. G. Brunton and M. C. Frame, *Nat. Rev. Cancer*, 2005, **5**, 505–515.
9 J. K. Slack-Davis, K. H. Martin, R. W. Tilghman, M. Iwanicki, E. J. Ung, C. Autry, M. J. Luzzio, B. Cooper, J. C. Kath, W. G. Roberts and J. T. Parsons, *J. Biol. Chem.*, 2007, **282**, 14845–14852.
10 V. M. Golubovskaya, C. Virnig and W. G. Cance, *Mol. Carcinog.*, 2008, **47**, 222–234.
11 J. Halder, Y. G. Lin, W. M. Merritt, W. A. Spannuth, A. M. Nick, T. Honda, A. Kamat, A. L. Y. Han, T. J. Kim, C. Lu, A. M. Tari, W. Bornmann, A. Fernandez, G. Lopez-Berestein and A. K. Sood, *Cancer Res.*, 2007, **67**, 10976–10983.
12 T. J. Liu, T. LaFortune, T. Honda, O. Ohmori, S. Hatakeyama, T. Meyer, D. Jackson, J. de Groot and W. K. Yung, *Mol. Cancer Ther.*, 2007, **6**, 1357–1367.
13 S. Bondock, S. Adel, H. A. Etman and F. A. Badria, *Eur. J. Med. Chem.*, 2012, **48**, 192–199.

14 V. D. Hande, T. S. Vasaitis, V. C. O. Njar, L. K. Gedia, R. Kataria, P. Chopra, D. Newman, R. Farquhar, Z. Guo, Y. Qui and A. M. H. Brodie, *J. Med. Chem.*, 2005, **48**, 2972–2984.
15 Z. Haddy, M. Toth and L. Somsak, *ARKIVOC*, 2004, **vii**, 140–149.
16 F. Liu, X. Q. Luo, B. A. Song, P. S. Bhadury, S. Yang, L. H. Jin, W. Xue and D. Y. Hu, *Bioorg. Med. Chem.*, 2008, **16**, 3632–3640.
17 G. Sahin, E. Palaska, M. Ekizoglu and M. Ozalp, *Farmaco*, 2002, **57**, 539–542.
18 S. A. Khan, P. Kumar, R. Joshi, P. F. Iqbal and K. Saleem, *Eur. J. Med. Chem.*, 2008, **43**, 2029–2034.
19 P. Sanna, A. Carta, L. Gherardini, M. Esmail and R. Nikookar, *Farmaco*, 2002, **57**, 79–87.
20 D. Liberman and N. Rist, *Chem. Abstr.*, 1957, **51**, 14137f.
21 V. Jakubkiene, M. M. Burbuliene, E. U. Drenait, V. Garaliene and P. Vainilavicius, *Pharmazie*, 2002, **57**, 610–613.
22 N. S. Habib, S. Fahmy, S. M. El-Khawas and T. Aziem, *Pharmazie*, 2000, **55**, 900–906.
23 A. R. Katritzky, D. O. Tymoshenko, K. Chen and A. A. Fattah, *ARKIVOC*, 2001, **2**, 101–108.
24 D. J. Li and Z. H. Ge, *Chem. Reagents*, 2005, **27**, 355–357.
25 J. Gautam, A. K. Kuldeep, S. Jagbir and K. V. Singh, *Biosci., Biotechnol. Res. Asia*, 2007, **4**, 325.
26 L. R. Zhang, Z. J. Liu and H. Zhang, *Bioorg. Med. Chem.*, 2012, **20**, 3615–3621.
27 D. W. Shen, L. M. Pouliot, M. D. Hall and M. M. Gottesman, *Pharmacol. Rev.*, 2012, **64**, 706–721.